



Research review paper

## 3D bioprinting for engineering complex tissues

Christian Mandrycky<sup>a,1</sup>, Zongjie Wang<sup>b,1</sup>, Keekyoung Kim<sup>b,\*</sup>, Deok-Ho Kim<sup>a,\*\*</sup><sup>a</sup> Department of Bioengineering, University of Washington, Seattle, WA 98195, USA<sup>b</sup> School of Engineering, The University of British Columbia, Kelowna, BC V1V 1V7, Canada

## ARTICLE INFO

## Article history:

Received 5 August 2015

Received in revised form 10 December 2015

Accepted 22 December 2015

Available online 23 December 2015

## Keywords:

Bioprinting

Bioink

Tissue engineering

3D printing

Hydrogel

Drug screening

Regenerative medicine

## ABSTRACT

Bioprinting is a 3D fabrication technology used to precisely dispense cell-laden biomaterials for the construction of complex 3D functional living tissues or artificial organs. While still in its early stages, bioprinting strategies have demonstrated their potential use in regenerative medicine to generate a variety of transplantable tissues, including skin, cartilage, and bone. However, current bioprinting approaches still have technical challenges in terms of high-resolution cell deposition, controlled cell distributions, vascularization, and innervation within complex 3D tissues. While no one-size-fits-all approach to bioprinting has emerged, it remains an on-demand, versatile fabrication technique that may address the growing organ shortage as well as provide a high-throughput method for cell patterning at the micrometer scale for broad biomedical engineering applications. In this review, we introduce the basic principles, materials, integration strategies and applications of bioprinting. We also discuss the recent developments, current challenges and future prospects of 3D bioprinting for engineering complex tissues. Combined with recent advances in human pluripotent stem cell technologies, 3D-bioprinted tissue models could serve as an enabling platform for high-throughput predictive drug screening and more effective regenerative therapies.

© 2015 Elsevier Inc. All rights reserved.

## Contents

1.	Introduction . . . . .	423
2.	Bioprinting techniques. . . . .	423
2.1.	Inkjet printing . . . . .	423
2.2.	Laser-assisted printing . . . . .	425
2.3.	Extrusion printing . . . . .	425
2.4.	Other technical approaches . . . . .	425
2.5.	Bioprinting CAD, modeling, and the printing process . . . . .	426
3.	Materials for bioprinting . . . . .	427
3.1.	Hydrogel bioink characteristics. . . . .	427
3.1.1.	Printability and crosslinkability . . . . .	427
3.1.2.	Mechanical properties . . . . .	427
3.1.3.	Biocompatibility and controllability of by-products and degradation. . . . .	427
3.2.	Bioinks . . . . .	427
3.3.	Cells. . . . .	428
4.	Applications of bioprinting . . . . .	428
4.1.	Vessels . . . . .	429
4.2.	Bone and cartilage . . . . .	429
4.3.	Neuronal tissues . . . . .	430
4.4.	Construction of drug screening systems. . . . .	431
5.	Present limitations and future prospects. . . . .	431
5.1.	Current limitations for bioprinting . . . . .	431
5.1.1.	Limitations of the current bioprinting approach . . . . .	431

\* Correspondence to: K. Kim, School of Engineering, University of British Columbia, EME 4263, 1137 Alumni Ave., Kelowna, BC V1V1V7, Canada.

\*\* Correspondence to: D.-H. Kim, Department of Bioengineering, University of Washington, N410G William H Foege Building, 3720 15th Ave NE, Box 355061, Seattle, WA 98195.

E-mail addresses: [keekyoung.kim@ubc.ca](mailto:keekyoung.kim@ubc.ca) (K. Kim), [deokho@uw.edu](mailto:deokho@uw.edu) (D.-H. Kim).<sup>1</sup> These authors contributed equally to this work.

5.1.2. Cell and material limitations . . . . .	431
5.2. Future prospects . . . . .	431
6. Conclusions . . . . .	432
Acknowledgement . . . . .	432
References . . . . .	432

## 1. Introduction

In the United States, one name is added to the organ transplant waiting list every 15 min (Abouna, 2008). While this list grows rapidly, less than one-third of waiting patients can receive matched organs from donors (Ozbolat and Yu, 2013). This growing deficit, however, is unlikely to be met by a supply of transplantable organs that has stagnated over the last decade (Bajaj et al., 2014). One of the most promising techniques to alleviate this organ shortage crisis is tissue engineering, the use of a combination of cell, engineering, and material methods to generate artificial tissues and organs (Langer and Vacanti, 1993). In tissue engineering, three strategies are used to replace or induce targeted tissues: (1) the use of cells alone, (2) the use of biocompatible biomaterials, (3) the use of a combination of both cells and biomaterials (Khademhosseini et al., 2006). These cells and biomaterials are combined into scaffolds through a variety of processes, which can generally be classified as either top-down, or bottom-up. In top-down approaches cells are often seeded sparsely and homogeneously in biomaterials shaped to resemble biological geometries. On the other hand, in bottom-up approaches modular units of cells and biomaterials are combined to form macro tissues. Top-down methods have been in wide use for years, however, these methods often cannot accurately control the distribution of cells, and fail to generate the appropriate extracellular matrix (ECM) (Khademhosseini et al., 2006). Without a proper ECM microenvironment, cells cannot function as tissues properly. This limitation is addressed in bottom-up approaches that build up tissues brick by brick via micro- and nano-technologies. As a result, cell distribution can be defined at the micrometer scale, which significantly improves the controllability of scaffold fabrication (Jiao et al., 2014). Motivated by developments in nanotechnology, techniques like self-assembly and soft-lithography have been applied to bottom-up tissue engineering (Kim et al., 2013, 2014a; Shapira et al., 2014). Among the micro-scale bottom-up techniques recently applied to tissue engineering, bioprinting, a form of additive manufacturing, has become one of the most promising and advanced fabrication methods (Table 1).

**Table 1**  
Comparison of tissue engineering methods.

	Assembly method			
	Bioprinting	Molding	Porous scaffolds	References
Materials	Natural and synthetic polymers High concentration cell solutions	Natural and synthetic polymers High concentration cell solutions Cell sheets	Natural and synthetic polymers  Ceramics  Metals 100 nm–1000 µm	Agarwal et al. (2013) and Skardal and Atala (2014)
Resolution	10–1000 µm	>500 nm		Kim et al. (2010), Lu et al. (2013) and Bajaj et al. (2014)
Advantages	Control of tissue geometry across a wide range of scales; rapid production of scaffolds; precise cell and material patterning	Accurate control of small (<100 µm) features; scaffold fabrication is rapid and molds are often reusable; gentle on encapsulated cells	Controllable material properties (e.g. porosity, modulus); wide range of materials available for use	Lu et al. (2013), Bajaj et al. (2014), Jiao et al. (2014) and Murphy and Atala (2014)
Disadvantages	Printing techniques may reduce cell viability or have unknown consequences; limited material selection due to crosslinking speed	Scaffolds are generally homogenous or require combination of multiple scaffolds to create patterns	Scaffold geometry is less controllable; technique may damage encapsulated cells or require seeding after assembly; less control of cell patterning	
Techniques	Extrusion Laser-assisted Inkjet Stereolithography	Cell sheet stacking Lithography Injection molding	Electrospinning Phase separation Freeze drying Self-assembly	Ballyns et al. (2008), Zheng et al. (2012), Lu et al. (2013) and Jiao et al. (2014)

In bioprinting, small units of cells and biomaterials are dispensed with micrometer precision to form tissue-like structures (Fig. 1). Unlike conventional 3D printing techniques that have been used to print temporary cell-free scaffolds for use in surgery (Bracci et al., 2013), bioprinting requires a different technical approach that is compatible with depositing living cells. The advantages of bioprinting include accurate control of cell distribution, high-resolution cell deposition, scalability, and cost-effectiveness. For those reasons, the development and subsequent applications of bioprinting have greatly increased during the last five years. In this review, we discuss the basic principles of bioprinting, including bioprinter device design, workflow, biomaterial options, and current and potential applications.

## 2. Bioprinting techniques

To date, no single bioprinting technique enables the production of all scales and complexities of synthetic tissues. The three major bioprinting techniques of inkjet, laser-assisted, and extrusion bioprinting each have specific strengths, weaknesses, and limitations. A concise comparison of these approaches is also provided in Table 2.

### 2.1. Inkjet printing

Inkjet bioprinting was the first bioprinting technology (Tuan et al., 2003) and is very similar to conventional 2D inkjet printing (Singh et al., 2010). A hydrogel pre-polymer solution with encapsulated cells (called a bioink) is stored in the ink cartridge. The cartridge is then connected to a printer head and acts as the bioink source during the electronically controlled printing process. During printing, the printer heads are deformed by a thermal or piezoelectric actuator and squeezed to generate droplets of a controllable size, as shown in Fig. 1B. The advantages of inkjet printing include: (1) low cost due to similar structure with commercial printers, (2) high printing speed conferred by the ability of the printer heads to support parallel work mode, and (3) relatively high cell viability (usually from 80% to 90%), as determined by many experimental results (Cui et al., 2012a, 2012b, 2013).

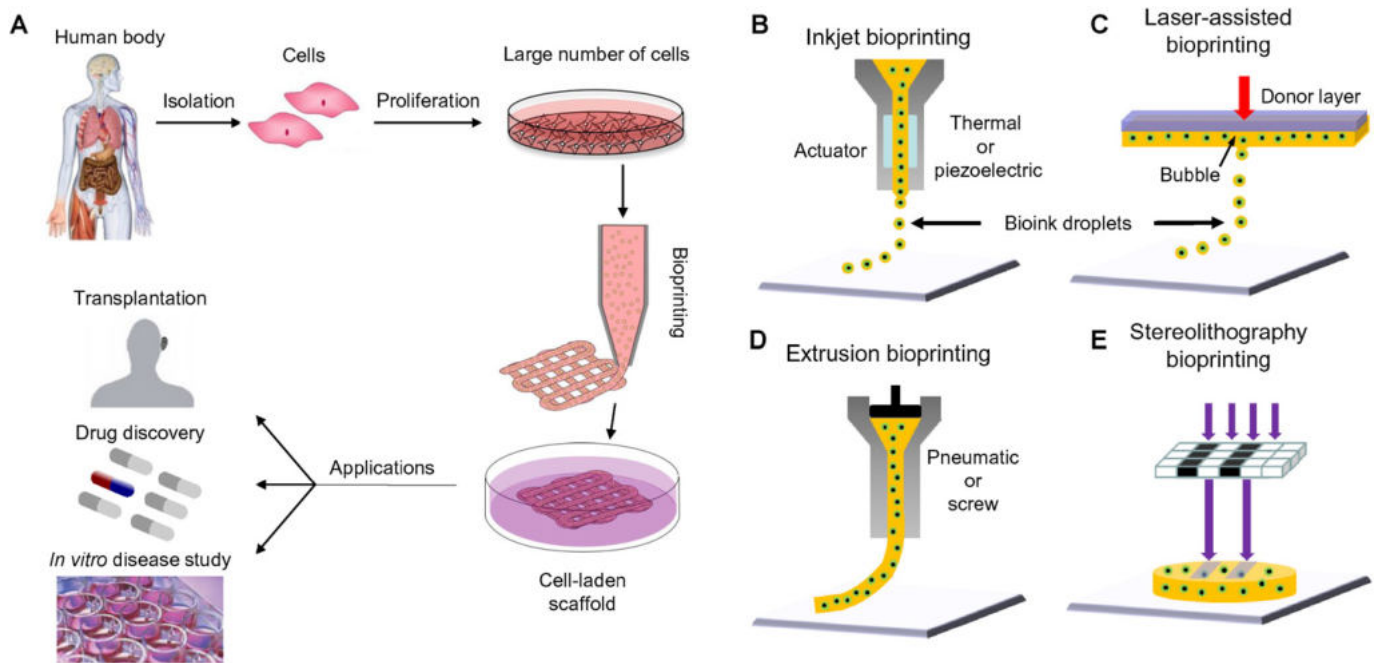


**Fig. 1.** Bioprinting process, techniques, and applications. (A) For human therapeutic applications, the typical workflow of bioprinting would involve the isolation and expansion of human cells prior to printing the desired cell-laden scaffold. These scaffolds could then ultimately be used as therapeutic devices themselves, as a testing platform for drug screening and discovery, or as an *in vitro* model system for disease. (B) Inkjet printers eject small droplets of cells and hydrogel sequentially to build up tissues. (C) Laser bioprinters use a laser to vaporize a region in the donor layer (top) forming a bubble that propels a suspended bioink to fall onto the substrate. (D) Extrusion bioprinters use pneumatics or manual force to continuously extrude a liquid cell–hydrogel solution. (E) Stereolithographic printers use a digital light projector to selectively crosslink bioinks plane-by-plane. In (C) and (E), colored arrows represent a laser pulse or projected light, respectively.

However, because current printer heads are based on micro-electromechanical system (MEMS) devices, there is a relatively small deformation generated by either thermal or piezoelectric actuation at the nozzle opening. As a result, MEMS-based printer heads cannot squeeze out high viscosity materials ( $>15$  mPa/s) and do not work well with bioinks with high cell density ( $>1 \times 10^6$  cells/mL). High cell density increases the average viscosity of bioinks, resulting in clogging of the head (Xu et al., 2005; Guillotin et al., 2010; Pepper et al., 2011, 2012). Recent research has highlighted another disadvantage of inkjet printing, named the settling effect (Pepper et al., 2011, 2012). When

bioinks are initially loaded into the ink cartridge, they are well mixed. Over the entire printing process, however, cells begin to settle in the cartridge, increasing the viscosity of the bioink and often clogging the printer head.

The simplest way to build inkjet bioprinter is to modify a commercial printer. HP 26 printer heads (Hewlett-Packard, Palo Alto, USA) were combined with a controller to print bioinks (Mattimore et al., 2010). Similar print heads were further integrated with a modified HP G3110 scanner (Hewlett-Packard, Palo Alto, USA) to build a low-cost bioprinter (~\$700) (Orloff et al., 2014). Such a low-cost system was achieved by

**Table 2**  
Comparison of four types of bioprinting techniques.

Parameters	Inkjet	Laser-assisted	Extrusion	Stereolithography	Reference
Cost	Low	High	Moderate	Low	Billiet et al. (2012), Ozbolat and Yu (2013), Orloff et al. (2014) and Ozbolat et al. (2014)
Cell viability	>85%	>95%	40%–80%	>85%	Xu et al. (2005) and Catros et al. (2011b)
Print speed	Fast	Medium	Slow	Fast	Xu et al. (2009b), Guillotin et al. (2010) and Murphy and Atala (2014)
Supported viscosities	3.5 to 12 mPa/s	1 to 300 mPa/s	30 mPa/s to above $6 \times 10^7$ mPa/s	No limitation	Guillemot et al. (2010), Chang et al. (2011) and Murphy and Atala (2014)
Resolution	High	High	Moderate	High	Ozbolat and Yu (2013)
Quality of vertical structure	Poor	Fair	Good	Good	Wang et al. (2015c)
Cell density	Low < $10^6$ cells/mL	Medium < $10^8$ cells/mL	High (cell spheroids)	Medium < $10^8$ cells/mL	Murphy and Atala (2014)
Representative materials for bioinks	Alginate, PEGDMA, Collagen	Collagen, Matrigel	Alginate, GelMA, Collagen	GelMA, GelMA-PEGDA hybrid hydrogel	Nahmias et al. (2005), Cui et al. (2012a), Xu et al. (2012), Kolesky et al. (2014), Ozbolat et al. (2014) and Wang et al. (2015c)
Reported applications	Tissue engineering (blood vessel, bone, cartilage, and neuron)	Tissue engineering (blood vessel, bone, skin, and adipose)	Tissue engineering (blood vessel, bone, cartilage, neuron, muscle, tumor) Controlled release of biomacromolecules Organ-on-a-chip	Tissue engineering (blood vessel and cartilage) Organ-on-a-chip	Chang et al. (2010), Ker et al. (2011), Gou et al. (2014) and Huang et al. (2014)

using commercial print heads as the dispenser, a scanner as a 2-axis servo stage, and free control software. The resolution of the servo stage was approximately 500  $\mu\text{m}$ , however, which is too coarse for micro-positioning. Additionally these print heads and cartridges are not capable of storing enough bioink to print large tissues, limiting the applications of this simple bioprinter.

Many efforts have been made to improve the stage resolution and enlarge the reservoir capacity. Screw-based servo stages with less than the 100  $\mu\text{m}$  resolution in each direction were used to provide sub-micrometer positioning (Nishiyama et al., 2009; Arai et al., 2011). External jugs and bottles were modified and connected to multiple print heads to increase the maximum bioink capacity. After adopting high accuracy stages and larger reservoirs, this inkjet bioprinter was able to achieve 10  $\mu\text{m}$  positioning accuracy and 20 picoliter droplet volume.

## 2.2. Laser-assisted printing

Laser-assisted printing originated from laser direct-write (Bohandy et al., 1986) and laser-induced transfer technologies (Duocastella et al., 2007; Kattamis et al., 2007). Fig. 1C shows a schematic of laser-assisted printing. The critical part of the laser-assisted printing system is a donor layer that responds to laser stimulation. The donor layer comprises a 'ribbon' structure containing an energy-absorbing layer (e.g., titanium or gold) on the top and a layer of bioink solution suspended on the bottom. During printing, a focused laser pulse is applied to stimulate a small area of the absorbing layer. This laser pulse vaporizes a portion of the donor layer, creating a high-pressure bubble at the interface of the bioink layer and propelling the suspended bioink. The falling bioink droplet is collected on the receiving substrate and subsequently crosslinked. Compared to inkjet printing, laser-assisted printing can avoid direct contact between the dispenser and the bioinks. This non-contact printing method does not cause mechanical stress to the cells, which results in high cell viability (usually higher than 95%). In addition, laser-assisted printing can also print highly viscous materials, and more types of bioinks can be used than in inkjet printing. These features of laser bioprinting are promising, but the side effects of laser exposure on the cell are not yet fully understood. Moreover, laser diodes with high-resolution and intensity are expensive compared to other nozzle-based printing methods, and control of the laser printing system is complex, limiting the technique's adoption.

Due to the high cost, there are few laser-assisted bioprinters, which are usually cumbersome and complex compared to other types of printers. A laser printing prototype was developed by combining optical laser sources with a lens (Nahmias et al., 2005). A more compact, high-throughput laser printing system was also built (Guillemot et al., 2010) and this system was further developed into a highly accurate version with 10  $\mu\text{m}$  resolution (Guillotini et al., 2010). In addition to the high equipment cost, laser-assisted printing is still immature because of unexplored parameters affecting the droplet size and quality. Instead of building prototypes of laser-assisted bioprinters, more researchers have focused on investigating the relationships between laser parameters, such as wavelength, intensity, and pulse time, with the quality of printed patterns (Duan et al., 2013; Duarte Campos et al., 2013).

## 2.3. Extrusion printing

Extrusion printing is a modification of inkjet printing. In order to print the viscous materials inkjet printers cannot deposit, extrusion printing uses either an air-force pump or a mechanical screw plunger to dispense bioinks, as shown in Fig. 1D. By applying a continuous force, extrusion printing can print uninterrupted cylindrical lines rather than a single bioink droplet. Almost all types of hydrogel pre-polymer solutions of varying viscosity as well as aggregates with high cell density can be printed with extrusion bioprinters.

While extrusion bioprinters can print a wider range of materials, they also expose the encapsulated cells to larger mechanical stresses that are thought to reduce cell viability (Khalil and Sun, 2007; Murphy and Atala, 2014).

Most existing commercial bioprinters, including the Bioplotter (EnvisionTec, Gladbeck, Germany) and NovoGen 3D Bioprinting platform (Organovo, San Diego, USA), are based on extrusion technology. Extrusion bioprinting provides good compatibility with photo, chemical and thermal crosslinkable hydrogels of very different viscosities at a reasonable cost (Khalil and Sun, 2007; Murphy and Atala, 2014). A typical extrusion printer, the multi-head tissue/organ building system from the Cho group, includes three-axis motion control with six dispensing heads, supporting up to six different bioinks (Lee et al., 2014). The substrate plate contains heating and cooling functions to control thermally sensitive hydrogels. Similar designs have been reported by two other groups (Chang et al., 2010; Bertassoni et al., 2014a). The latest versions of extrusion printers include tissue–vessel parallel printing (Ozolat et al., 2014) and parallel multi-bioink printing (Kolesky et al., 2014).

Dispensers in current extrusion systems have a few differences (Khalil and Sun, 2007). Pneumatic micro nozzles powered by compressed gases support a wider range of viscosity, but have difficulty precisely controlling the deposited mass. Screw-based nozzles can print without inlet air and are much cheaper, but they experience problems in high viscosity dispensing.

## 2.4. Other technical approaches

While these three printing methods are most commonly used by bioprinting researchers, the bioprinting paradigm itself has been challenged and novel printing methodologies remain under investigation. Rather than directly printing tissues, Miller et al. (2012) used a pneumatically controlled syringe to print molten sugar glass in the shape of a desired vascular network. Once printed, this artificial vascular network was embedded within a variety of hydrogels and could then be dissolved to form open channels within cross-linked tissues. While this approach sacrificed the ability to carefully control the deposition of cells within the bulk matrix, it enabled previously unachieved engineered vascular complexity in a synthetic tissue.

Stereolithography has also been modified for bioprinting purposes (Fig. 1E) (Gauvin et al., 2012; Gou et al., 2014). Like laser-assisted printing, stereolithography bioprinters use light to selectively solidify a bioink in a layer-by-layer process that additively builds up objects (Fig. 2A). These printers use a digital light projector to cure bioinks plane-by-plane and have several advantages over traditional bioprinting methods. No matter how complex pattern in one layer is, the printing time is the same because the entire pattern is projected over the printing plane. As a result, the printer only needs a moveable stage in a vertical direction, which significantly simplifies the control of the printer. This reported stereolithography bioprinting system can achieve 100  $\mu\text{m}$  resolution and printing times less than 1 h (Gauvin et al., 2012; Gou et al., 2014) while maintaining very high cell viability (>90%). Fig. 2B–E show the woodpile and hexagonal structures printed by the stereolithography system. The fluorescent images of the hexagonal structures encapsulated with human umbilical vein endothelial cells (HUVECs) are given in Fig. 2F–H. Recently, a commercial beam projector was adopted as the light source, providing an inexpensive solution (< \$1,000) for stereolithography bioprinting (Wang et al., 2015c). This system was able to print hydrogel patterns with 50  $\mu\text{m}$  resolution. A recent advance in stereolithographic 3D printing technology by the DeSimone group (Tumbleston et al., 2015) referred to as "continuous liquid interface production (CLIP)" dramatically improved both resolution and printing time for some materials. While this has not yet been applied to bioprinting, it may be an approach that enables the formation of more complex tissue architectures.



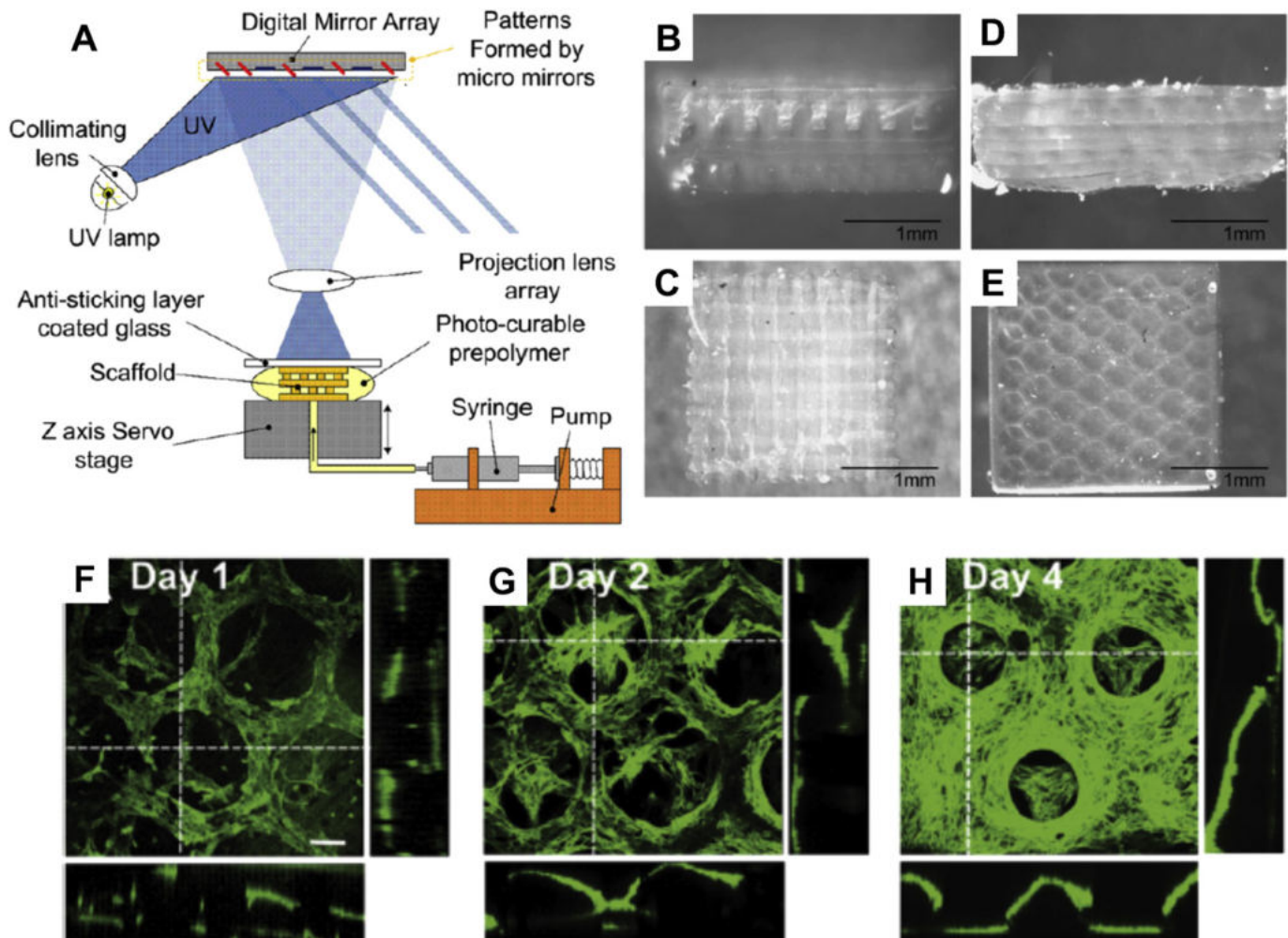


**Fig. 2.** Stereolithographic bioprinting. (A) Schematic illustration of a stereolithography system (Gauvin et al., 2012). (B)–(E) The side view of woodpile (B) and hexagonal (D), as well as the top view of woodpile (C) and hexagonal (E) structures generated by their stereolithography system. (F)–(H) 3D confocal images showing the proliferation of encapsulated HUVEC cells in day 1 (F), day 2 (G) and day 4 (H) (scale bar: 100 μm).

### 2.5. Bioprinting CAD, modeling, and the printing process

Bioprinters cannot print without instructions. To successfully create bioprinted tissues, it is necessary to generate the printing paths, select appropriate bioinks, control the bioprinter and perform quality control after printing (Murphy and Atala, 2014). The typical bioprinting process is as follows: (1) designers draw the printing geometry and manually verify its feasibility; (2) designers select appropriate cell types and hydrogels, and load the bioinks into the bioprinting system (3) through control language and protocols, such as RS 274 (G-Code, Massachusetts Institute of Technology, Cambridge, USA) and LabView (National Instruments, Austin, USA), the designed paths are sent to the bioprinting system; (4) the bioprinter builds structures by depositing bioinks under the control of a computer; (5) bioprinted tissues are checked manually *via* microscopy after bioprinting. After the bioprinting process, successfully printed constructs are transferred to an incubator for culturing. The bioprinting process is not currently highly automated and many manual operations at a variety of steps can result in slow processing speeds and increase the chance for mistakes and errors. To ensure printing quality and to improve the printing process, many researchers have investigated computer-aided design (CAD) and modeling technology for bioprinting. These CAD techniques can utilize computer automation systems to assist and accelerate the design process.

Bioprinting models, like models used in conventional rapid prototyping, are often converted to the STereoLithography (STL) file format as an intermediate between model and print path generation (Mironov et al., 2009; Mondy et al., 2009). These files contain accurate surface information of complex 3D geometries, and can be designed *via* graphic user interfaces, or created from clinical images, including those from magnetic resonance imaging (MRI) and computed tomography (CT) (Keriquel et al., 2010; Arai et al., 2011). In a process analogous to histologic sectioning, printing paths are created by “slicing” these STL model into layers and creating bioprinter toolpaths that trace out the perimeter and interior features of each slice. The thickness of these layers is often referred to as the resolution of a particular printer and is usually in the range of 100–500 μm depending on the machine and material used. These toolpaths are the instructions read and executed by the bioprinter for each layer and can include material selections. Layers are formed sequentially and stacked as the model is built up in an additive process forming a 3D object from a collection of 2D layers. All other things being equal, smaller resolutions are associated with higher quality and longer print times.

Clinical images can provide information regarding the *in vivo* tissue distribution of patients, and anatomically realistic tissue geometries can be determined *via* image processing. Clinical image-based STLs therefore have the potential to become the starting point for on-demand tissue production in the future. In addition, a smart program

was coded for planning and optimizing bioprinting experimental design (Weiss et al., 2005). In summary, the introduction of Bio-CAD techniques has significantly improved the automation of bioprinting path generation.

Computer aided techniques, known as bio-computer-aided-manufacturing (Bio-CAM), also play an important role during and after bioprinting. Bio-CAM aims to predict the feasibility of the fabrication process by simulating relevant physical models on computers. To simulate bioprinting, both classical formula calculations and the finite element method (FEM) are applied. Currently, the most widely used physical model for bioprinting is laminar multi-phase flow. Although this model is oversimplified, ignoring complex issues generated by the inclusion of cells, simulations are still helpful for checking and optimizing the feasibility of specific designs. Many researchers are already attempting to model bioprinting results with the corresponding printing parameters. For extrusion printing, relationships between dispensing pressure, printing time, and nozzle diameter have been tested and modeled (Yu et al., 2013). Cell settling effects in inkjet printers, which are highly related to clogging and viscosity, change during printing and were modeled by both analytical and finite element methods (FEM) (Pepper et al., 2011, 2012). For laser printing, the effects of laser energy, substrate film thickness, and hydrogel viscosity on the viability of cells (Catros et al., 2011b), as well as droplet size (Duocastella et al., 2007; Mézel et al., 2010; Gruene et al., 2011b), cell differentiation (Gruene et al., 2011a), and cell proliferation (Gruene et al., 2011a) have been investigated. Some researchers also focused on post-printing modeling of cellular dynamics (McCune et al., 2014), fusion (Yang et al., 2012, 2013; Sun and Wang, 2013; Thomas et al., 2014), deformation (Sim et al., 2007) and stiffness (Tirella et al., 2011; Mobed-Miremedi et al., 2012), as well as modeling of the typical types of printed tissues, including tumors (Zhao et al., 2014) and soft tissues (Zhang et al., 2013). Bio-CAM research not only provides a fast way to check design feasibility, but also gives designers a chance to better understand the physical and chemical principles governing printing. With the integration of Bio-CAD and Bio-CAM, an advanced design flow for bioprinting begins to take shape. Bio-CAD can accelerate the speed of the whole bioprinting process, and Bio-CAM can guarantee the quality of what is printed.

### 3. Materials for bioprinting

Bioinks typically consist of a hydrogel pre-polymer solution and cells. The desired properties of hydrogels are presented at the beginning of this section, and the characteristics of various types of crosslinkable hydrogels are summarized. Resources for the cells and materials used in bioprinting applications are briefly reviewed at the end.

#### 3.1. Hydrogel bioink characteristics

Hydrogels play an essential role in bioprinting. They not only have direct contact with cells to provide structural support, but they also dominate the chemical and physical properties of bioinks (Williams, 2008). Ideally, hydrogels used for bioprinting should be characterized by the properties described below.

##### 3.1.1. Printability and crosslinkability

Printability refers to the relationships between bioinks and substrates that results in printing an accurate, high-quality pattern (Murphy and Atala, 2014). In bioprinting, printability is usually associated with surface tension, which is measured by the contact angles between two media. Research has shown that the surface tension of supporting structures has significant and profound implications on cell attachment and development (Discher et al., 2005). To form 3D scaffolds, the printed hydrogel pre-polymer solution should not be too flat on the substrate. This means that the hydrogel pre-polymers are expected to maintain tension in the vertical direction and have a large

contact angle with the substrate. Since glass slides and petri dishes are the most commonly employed substrates, ideal hydrogel pre-polymer solutions should be able to build highly vertical structures after printing on glass and plastic substrates. Unfortunately, most of the glass slide substrates have poor contact angles. This problem can be solved by coating the substrates with a thin layer of material, such as 3-(trimethoxysilyl)propyl methacrylate (TMSPMA) (Zhang et al., 2008), to enhance their hydrophobicity before printing (Bauer et al., 2012; Nikkhab et al., 2012).

Printability is also influenced by how easily materials can be crosslinked. The three types of bioprinting technologies currently available are only capable of dispensing liquid materials and consequently hydrogels must be in liquid or paste-like form during printing. To accommodate different cell densities and printing technologies, the viscosity of the hydrogel pre-polymer solutions should be controllable over a wide range. At odds with this condition, bioinks must form a quasi-scaffold structure to support cell proliferation after printing. These conditions have effectively limited hydrogel pre-polymer solutions to either photo (Weiner et al., 2007; Nichol et al., 2010), chemically (Li et al., 2005; Glowacki and Mizuno, 2008; Liu et al., 2009; Balakrishnan et al., 2012; Araujo et al., 2014), or thermally (Gao et al., 2012; Wu et al., 2012) crosslinkable polymers (Murphy et al., 2013; Bajaj et al., 2014).

##### 3.1.2. Mechanical properties

Hydrogels should maintain sufficient mechanical properties after polymerization to provide the cells with a stable environment for attachment, proliferation and differentiation (Limpanuphap and Derby, 2002; Murphy et al., 2013). These mechanical properties include strain, shear stress, compressive modulus and mass swelling ratio. It is well understood that cell adhesion is significantly affected by the dynamic interactions between cells and hydrogels (Dou et al., 2012; Benson et al., 2014). In fact, mechanical properties are considered to be highly essential for soft tissues, such as cartilage and skin, because the functions of such tissues mainly rely on their mechanical properties (Hutmacher, 2000; Kim et al., 2012).

##### 3.1.3. Biocompatibility and controllability of by-products and degradation

Biocompatibility refers to the ability of a material to perform with an appropriate host response in a specific situation (Hobkirk, 1988). In general, for *in vitro* applications, biocompatibility requires that the material itself is not harmful to cell proliferation and has the ability to provide proper binding with cells (Williams, 2008). For *in vivo* applications, biocompatibility adds the requirement that the material can be degraded by or integrated with the ECMs of cells without generating harmful by-products or having negative interactions with cells (Williams, 2008). It is desirable for implanted tissue to eventually fuse with other *in vivo* tissues. Therefore, hydrogel scaffolds need to be degraded or integrated with the *in vivo* ECM environment and hydrogels with a natural and controllable degradation rate which is similar to the ECM growth rate is highly desired (Murphy and Atala, 2014).

#### 3.2. Bioinks

From the perspective of hydrogel design, there are basically two types of hydrogels: those based on natural polymers and those based on synthetic polymers (Zorlutuna et al., 2013). Natural hydrogels include polymers existing in ECM components, such as gelatin, collagen, laminin and fibronectin, as well as other natural polymers such as alginate, chitosan and silk fibroin. Interactions between natural hydrogels and cells have been well investigated (Zorlutuna et al., 2013). Synthetic polymers, unlike natural polymers, are made through chemical synthesis and are typically more controllable in terms of their chemical and mechanical properties (Zhu and Marchant, 2011). Their interactions with and effects on cells, however, have not yet been studied

systematically (Zorlutuna et al., 2013). Natural polymers are widely used in bioprinting research, but some researchers have used a combination of natural and synthetic polymers (Schuurman et al., 2011; Xu et al., 2013).

Decellularized extracellular matrices have been an increasingly promising material in tissue engineering as decellularization protocols have steadily improved. Recently, Pati et al. (2014) showed that dECMs from three tissues could be solubilized into bioinks and bioprinted. While many bioinks are compositionally simple, dECM bioinks contain the diverse array of ECM components characteristic of different tissues and as a result, more closely resemble the native tissue. Although the mechanical properties of dECM bioinks do not mirror the original tissue, they represent a promising addition to the bioinks available in bioprinting.

On the synthetic side, there is significant interest in developing conductive biomaterials (Balint et al., 2014). Recently Jakus et al. (2015) developed a printable high-content graphene:polyactide-co-glycolide bioink with high conductivity (800 S/m). Scaffolds printed with this material were able to support the growth of human mesenchymal stem cells (hMSCs) and have interesting possible applications in both biomedical devices and biologic scaffolds where enhanced conductivity is desirable. For example, conductive tracks through scaffolds could be pre-patterned in printed tissues simply by changing the bioink. This would complement a previously demonstrated method for installing these tracks by using  $\alpha$ -hemolysin containing droplets (Villar et al., 2013). For a more complete discussion of existing biomaterials for bioprinting as well as the interaction and trade-off between desired hydrogel properties, we refer the reader to recent reviews (Bajaj et al., 2014; Skardal and Atala, 2014).

### 3.3. Cells

To form a highly mimetic tissue or organ on a macro scale, bioprinted cells must proliferate. Two main factors are considered when selecting cells for bioprinting: how closely the bioprinted cells can mimic the physiological state of cells *in vivo*, and to what degree

the bioprinted cells can maintain or develop their *in vivo* functions under optimized microenvironments (Murphy and Atala, 2014). Artificial tissues are seeded by either printing functional primary cells with supporting cells (Keriquel et al., 2010; Cui et al., 2012a; Duan et al., 2013; Michael et al., 2013; Xu et al., 2013; Zhang et al., 2013; Dolati et al., 2014) or printing progenitors or stem cells for further differentiation (Gruene et al., 2011a; Xu et al., 2011; Duarte Campos et al., 2013; Hong et al., 2013; Owens et al., 2013; Visser et al., 2013). Direct printing of primary cells can rapidly increase the complexity of bioprinting. Since multiple types of cells embedded within the same or different hydrogels need to be printed in parallel, many bioinks need to be prepared for each print. Real-time alignment and printing step control are complicated by using many bioinks as each switch between bioinks has the possibility to introduce error into the bioprinting process. Printing with stem cells will usually reduce the total number of bioinks used for a given print, but also adds its own set of complications. Additional bioink formulations with different growth factor and small molecule signals may be desirable to attempt to guide site-specific differentiation. Even without this kind of approach, there is added difficulty in post-printing culture as growth factors and other differentiation stimulators must be deposited precisely to ensure the control of differentiation, especially when vascularization is desired.

Reliable cell sourcing poses a perennial problem to bioprinting. For clinical applications, cells for bioprinting would ideally be isolated from the patients themselves to avoid negative immune responses (Ozbolat and Yu, 2013). Because not all types of cells can regenerate after damage (e.g. cardiac muscle cells), stem cells (e.g. adipose derived stem cells) with the ability to proliferate and differentiate into the desired cell types are the most promising cell source. Examples of some of the cell types and organ systems targeted by recent bioprinting publications are presented in Table 3.

## 4. Applications of bioprinting

In this section, the current applications of bioprinting are reviewed in terms of several popular tissue types and its role in drug screening.

**Table 3**  
Examples of bioprinted tissues and organs.

Tissue	Cell sources	Materials	Printing method	Reference
Vessel	Smooth muscle cells	Carbon nanotube encapsulated alginate	Extrusion	Dolati et al. (2014)
	Smooth muscle cells and aortic valve leaflet interstitial cells	Gelatin and alginate	Extrusion	Duan et al. (2013)
	Human umbilical vein endothelial cells (HUVEC)	PEG-DA, Matrigel, fibrin gel, alginate, agarose, and GelMA	Extrusion	Miller et al. (2012) and Kolesky et al. (2014)
	Rat heart endothelial cells Ea.hy926 endothelial cells	Alginate Nano-hydroxyapatite (n-HA)	Extrusion Laser-assisted	Khalil and Sun (2009) Catros et al. (2011b)
Bone	Fibroblasts (L929), mouse endothelial cells and human mesenchymal stem cells HUVEC	Acrylated hyaluronic acid-PEG (HA-PEG), and Matrigel GelMA	Inkjet	Hong et al. (2013)
	Mouse osteoblastic cells MG-63 cells	n-HA Alginate	Stereolithography Inkjet Extrusion	Gauvin et al. (2012) Keriquel et al. (2010) Loozen et al. (2013)
	Human osteoprogenitor cells	n-HA	Laser-assisted	Catros et al. (2011a)
Cartilage	Patient's cartilage	Poly(ethylene glycol) dimethacrylates (PEGDMA)	Inkjet	Cui et al. (2012a)
	Minced cartilage cells	Poly ( $\epsilon$ -caprolactone) (PCL), and fibrin-collagen hydrogels	Inkjet	Xu et al. (2013)
Skin	Equine chondrocytes and mesenchymal stromal cells (MSCs)	PCL, GelMA, and GelMA-gellan hydrogels	Extrusion	Visser et al. (2013)
	Human meniscus cells	GelMA	Stereolithography	Grogan et al. (2013)
Neuronal tissue	NIH3T3 fibroblast, HaCaT keratinocytes	Collagen	Laser-assisted	Michael et al. (2013)
	Mouse bone marrow stem cells	Collagen, and agarose	Extrusion	Owens et al. (2013)
Skeletal muscle	Embryonic stem cells	N/A	Inkjet	Xu et al. (2011)
	C2C12 mouse myoblasts	Polyurethane (PU), and PCL	Extrusion	Merceron et al. (2015)
Tumor	C2C12 mouse myoblasts	Alginate, and gelatin	Extrusion	Zhang et al. (2013)
	Hela cells	Gelatin–alginate–fibrinogen hydrogel	Extrusion	Zhao et al. (2014)
Adipose tissue	Adipose derived stem cells	Alginate	Laser-assisted	Gruene et al. (2011a)



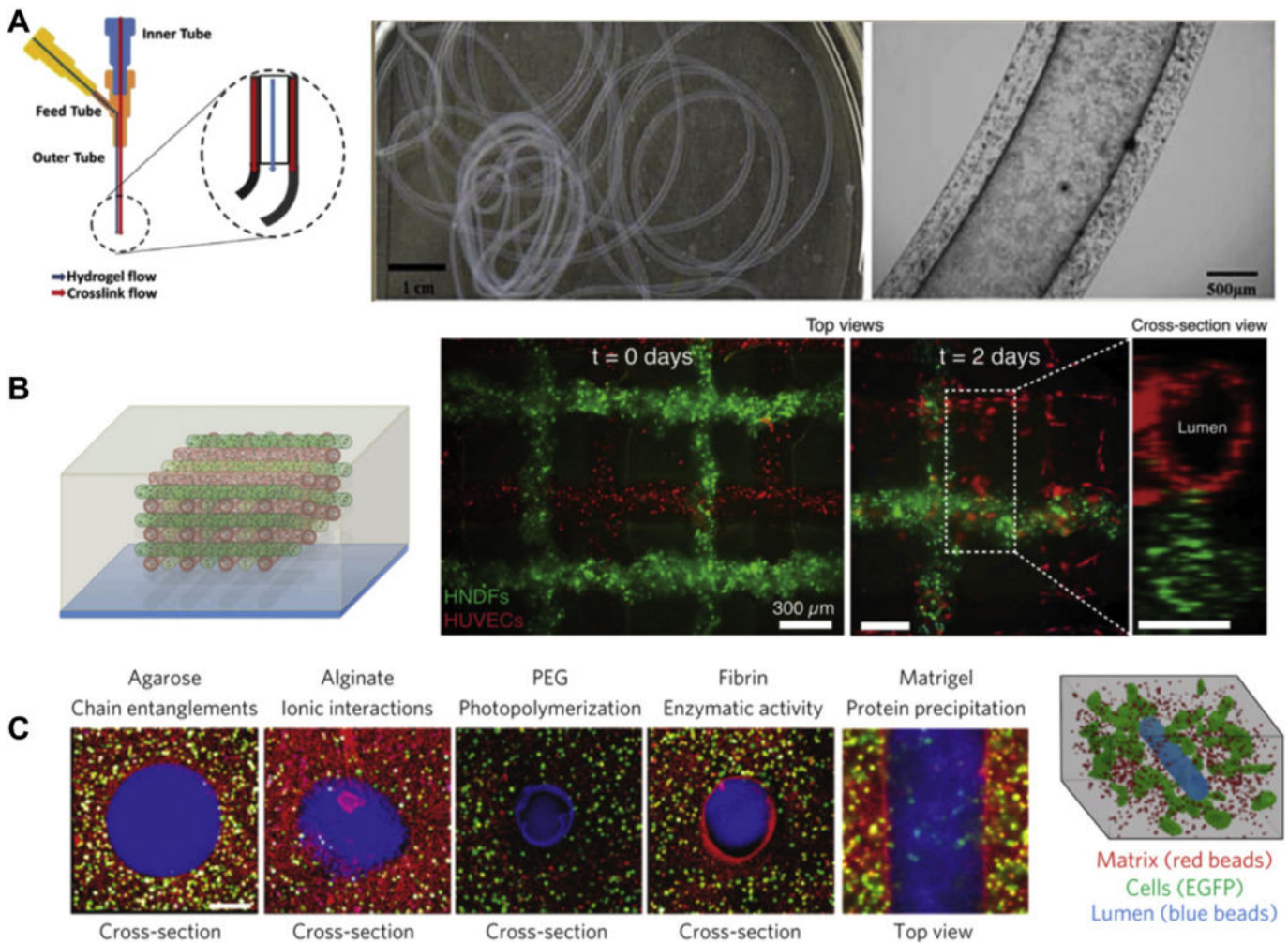


**Fig. 3.** Bioprinting strategies for vascularization. (A) Fabrication of long (>1 m) vascular conduits using a coaxial nozzle system yielding internal lumen diameters below 1 mm (Dolati et al., 2014). (B) Pluronic F127 as a sacrificial bioink to form open lumens (red) while concurrently printing encapsulated cells around the vessels (green) (Kolesky et al., 2014). (C) Carbohydrate glass to cast vascular features into a variety of hydrogels, forming perfusable vessels that support cell growth (Miller et al., 2012). Figure adapted from Miller et al. (2012), Dolati et al. (2014), and Kolesky et al. (2014).

#### 4.1. Vessels

While the ability to create vascular features in bioprinted tissues is often limited, novel bioprinting techniques may resolve this problem. Dolati et al. (2014), for example, utilized a coaxial nozzle system to print vascular conduits more than a meter long (Fig. 3A). These carbon nanotube reinforced alginate conduits were perfusable and supported the growth of human coronary artery smooth muscle cells within the matrix. Using this technique, the authors were able to fabricate conduits with diameters in the sub-millimeter range, but did not show an ability to print closer to capillary diameters. Another possible solution is to add magnetically controlled nanoparticles to bioinks and use these to print vessels. With this technique the position of the vessels within tissues could then be controlled by applying a magnetic field (Mironov et al., 2008; Talelli et al., 2009). However, further research is needed to determine the efficiency and the potential effects of magnetic particles on cells and ECM. To reduce the size of vascular channels and to incorporate them directly into printed tissues, others have employed sacrificial inks to some success. Kolesky et al. (2014) used a Pluronic F127 fugitive bioink to print channels as small as 45  $\mu\text{m}$  and were able to subsequently endothelialize them with HUVECs. This approach, combined with printing fibroblasts encapsulated in a gelatin methacrylate bioink, yielded multicellular bioprinted constructs (Fig. 3B). Once the

constructs were printed and crosslinked, the temperature was lowered to 4  $^{\circ}\text{C}$  to liquefy and remove the Pluronic F127, leaving behind open vascular channels ready to be seeded. Previously, Miller et al. (2012) encapsulated and dissolved printed carbohydrate glass in various bulk extracellular matrices to form seedable channels as small as 150  $\mu\text{m}$  (Fig. 3C). Rather than dissolving away the sacrificial material, Bertassoni et al. (2014b) cast hydrogels around printed agarose fibers and then aspirated or manually removed the fiber. The resulting lumen were perfusable and HUVECs could form an endothelial monolayer. These sacrificial techniques are exciting advances that may simplify not only the pre patterning of vascular features in bioprinted tissues, but also the speed at which large tissues can be printed.

#### 4.2. Bone and cartilage

The bone engineering space is interesting in that both conventional and bioprinting are poised to influence the field. Made to order metal 3D printed devices (Hsu and Ellington, 2015), 3D printed models for surgical planning (Pietrabissa et al., 2015; Scawn et al., 2015), and 3D printed tools (Burlison et al., 2015) highlight some of the current and future biomedical applications of conventional 3D printing technologies. Bioprinting techniques have also been applied to bone tissue engineering. Yao et al. (2015) used anatomic data from CT scans of rabbits to



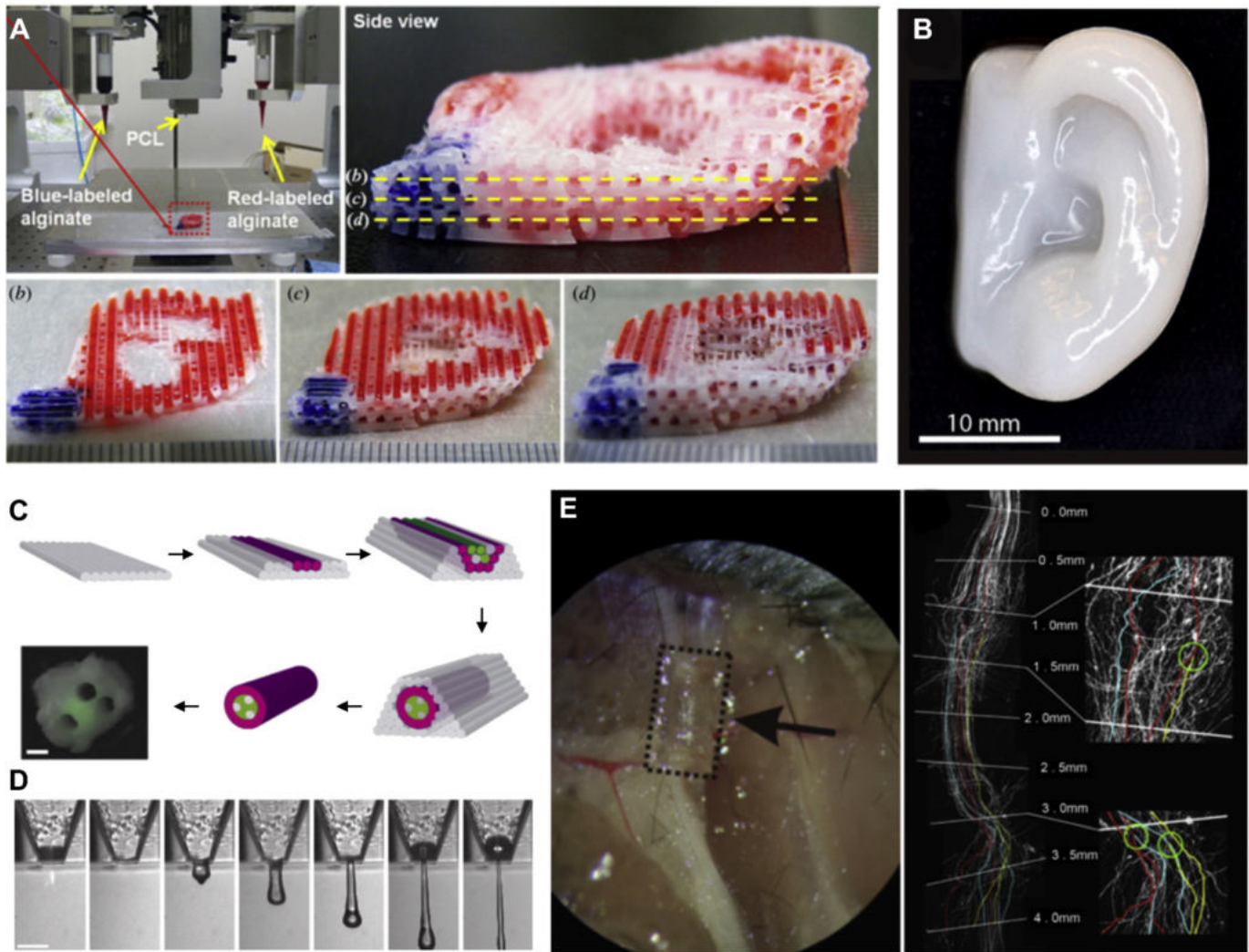


**Fig. 4.** Examples of bioprinted tissues and organs. (A) Printed ear-shaped PCL and alginate scaffolds with bioinks localized to certain tissue regions (Lee et al., 2014). (B) Cartilaginous ear scaffolds printed using a novel nanocellulose–alginate bioink supported human chondrocytes (Markstedt et al., 2015). (C) Fabrication of a synthetic nerve graft by printing cell-dense tubes of Schwann cells and BSMC (Owens et al., 2013). (D) Demonstration of the feasibility of printing mouse ganglion and glial cells (Lorber et al., 2014). (E) Printed PEG-based guidance conduits for nerve repair studies, showing their biocompatibility and efficacy (Pateman et al., 2015). Figure adapted from Owens et al. (2013), Lee et al. (2014), Lorber et al. (2014), Markstedt et al. (2015), and Pateman et al. (2015).

print and test polycaprolactone–hydroxyapatite scaffolds which supported physiologically relevant loads. Wang et al. (2015a) printed poly(propylene fumarate) porous scaffolds, characterized the degradation process over a 224 day period, and showed the printed scaffolds were suitable for bone tissue engineering applications. Pati et al. (2015) enhanced the osteogenic potential of 3D–printed PCL/PLGA/ $\beta$ -TCP scaffolds by using human nasal inferior turbinate tissue-derived mesenchymal stromal cells to deposit bone-like ECM. After a brief culture period, the scaffolds were decellularized and then investigated both *in vitro* and *in vivo* where they showed improved osteoinductive and osteoconductive properties.

Cartilaginous tissues have also been an area of interest in tissue engineering (Tatman et al., 2015). Kundu et al. (2013) printed alginate encapsulated chondrocytes with a supportive PCL structure and *in vivo* experiments suggested cartilage production. Lee et al. (2014) printed a PEG and PCL construct containing chondrocytes and showed that this material mixture could be used to print ear-shaped constructs (Fig. 4A). Similarly, Markstedt et al. (2015) developed a novel nanocellulose–alginate bioink with desirable printing properties. This ink supported the culture of human nasoseptal chondrocytes in printed tissues and could also be printed into complex shapes (Fig. 4B).

Collectively, studies like these highlight the promise of bioprinting to produce unique 3D structures suitable for bone and cartilage tissue engineering.

#### 4.3. Neuronal tissues

Bioprinting nervous tissue is another application that has been explored by researchers. Large synthetic tissues will need to integrate with the host nervous system, and bioprinting may be a means to generate new nervous tissue or to enhance the innervation of tissue engineered constructs. Owens et al. (2013) printed a synthetic nerve graft using cells alone. Isolated mouse bone marrow stem cells and Schwann cells were cast into 500  $\mu$ m diameter tubes and then loaded into a bioprinter which extruded discrete tubes to form a dense nerve conduit of Schwann cell tubes surrounded by mouse bone marrow stem cell tubes for use in animal studies (Fig. 4C). These early stage proof-of-principle printed grafts performed similarly to control tissues and remain promising as the methodology is refined and improved. Lorber et al. (2014) also provided important validation on the feasibility of printing cells of the nervous system, showing rat retinal ganglion cells and glia can be used in inkjet printing systems (Fig. 4D). Pateman et al.

(2015) used a microstereolithographic technique to print PEG-based nerve guidance conduits for nerve repair studies (Fig. 4E). Printed conduits had a finer resolution than those made through previously reported methods and performed comparably to autograft controls.

#### 4.4. Construction of drug screening systems

Bioprinting is also promising in the design of drug screening systems. Compared to manual methods, bioprinting can deposit cells uniformly on the surface of micro devices. Such uniformity is highly desirable for testing and screening the interactions between cells and drugs (Huh and Kim, 2015; Nam et al., 2015). Existing examples of bioprinted drug testing platforms include those for the liver (Snyder et al., 2011). Chang et al. (2010) developed an air-pressure based extrusion bioprinter to prototype a drug testing platform for the liver with alginate encapsulated immortalized hepatocytes. In this system, the authors were able to show differential drug metabolism. Snyder et al. (2011) expanded on this system by printing microfluidic channels in a co-culture system of liver and mammary cells to investigate tissue damage from radiation. Bioprinting has also been used to seed cell layers uniformly on each side of the interface of micro devices for the formation of organ-on-a-chip devices (Chang et al., 2010). Organ-on-a-chip systems mimic parts of typical organ functions to investigate the interactions between drugs and their potential effects on tissues (Wang et al., 2015b). Bioprinting may play an important role in organ-on-a-chip technology, given it is a practical solution for the formation of uniform and highly controllable tissue layers at low cost.

## 5. Present limitations and future prospects

### 5.1. Current limitations for bioprinting

#### 5.1.1. Limitations of the current bioprinting approach

Although these three common bioprinting techniques have different printing principles and features, there are a few limitations to the typical bioprinting process as it stands today. All three techniques are based on a layer-by-layer printing method, which generally have difficulty printing complex hollow structures. In the simplest case of printing with a single material, each layer must be connected and mechanically supported as it is printed. When voids are introduced in one layer, subsequent layers that deposit material over the void may collapse causing a cascade of offset features and inaccurate geometries. One possible solution to this problem is to incorporate a sacrificial material, which is a method widely employed in the fabrication of suspended structures in MEMS (Taylor et al., 2013; Bertassoni et al., 2014b). This sacrificial material provides the mechanical support each layer needs during fabrication and is then removed from the completed object in a post-processing step. This approach has been taken by several groups using several fugitive materials, including carbohydrate glass (Miller et al., 2012), Pluronic F-127 (Kolesky et al., 2014) and gelatin microparticles (Hinton et al., 2015). The introduction of extra materials, however, can increase the complexity of the printing process as the bioprinting platform must support rapid material exchanges or multiple nozzles loaded with different inks. Sacrificial materials must be printable under conditions compatible with non-sacrificial biomaterials and cells, and their method of removal and breakdown products must be cytocompatible. These difficulties have likely limited the development and adoption of new sacrificial materials.

The lack of reliable methods to print pre-vascularized tissues is a hurdle that cannot be overlooked. This problem is not unique to bioprinting, but bioprinting is unique in its ability to create large tissues with high metabolic demands relatively quickly. Many of the small-scale tissues researchers currently print can survive through diffusion alone, but full-scale organs and large tissue constructs will require an embedded vasculature as well as mechanically robust conduits to connect to host arteries and veins. Small bioprinted tissues may take

only minutes or hours to print, but the question of cell viability both within a pre-polymer bioink and within the polymerized early regions of large multi-day prints must be addressed. Self-assembly of vascular features is too slow a process to rely on when there is the threat of necrosis in partially assembled tissues still sitting on the printer. These sacrificial techniques represent the most promising approach in the current bioprinter's toolbox, but innovation could lead to better printed tissues.

In addition to the difficulty in fabricating hollow vascular features, bioink preparation can take several days to weeks due to cell culturing and biomaterial synthesis (Murphy and Atala, 2014). Once fully prepared, the working time of bioinks may also become an issue. This issue of time may be overcome by incorporating additional features into the bioprinter that support the maintenance of partially printed structures, the development of increasingly parallel bioprinters (e.g. multiple print heads working simultaneously) or other refinements to the printing process (e.g. CLIP; Tumbleston et al., 2015). Faster bioprinters with higher resolution would be poised to solve some of the problems faced by modern technology.

#### 5.1.2. Cell and material limitations

Material selection remains a major concern and limitation for bioprinting. More biomimetic materials like dECM bioinks often lack the mechanical strength to be the sole material in printed tissues, requiring support from stronger but less bioactive inks, like PCL (Ousterout et al., 2013). Tunable bioinks with a wide range of material properties could be a solution to this problem and may be achievable through the creation of new composite mixtures to enhance crosslinking or incorporate other desirable features while maintaining the properties of the base bioink. Poly(ethylene glycol) (PEG) has received attention because of its tunable mechanics (Zustiak and Leach, 2010; Kim et al., 2014b) and represents a suitable component for composite bioinks. The Khademhosseini group developed PEG:gelatin methacrylate (PEG:GelMA) and carbon nanotube-incorporated photocrosslinkable gelatin methacrylate (CNT:GelMA) composites with tunable mechanical and degradation properties that could have such applications (Shin et al., 2013). Similarly, the West group (Zhang et al., 2015) developed a low molecular weight–high molecular weight PEG composite which could mimic the anisotropy of heart valve leaflet moduli. These kinds of composites further expand the options available to researchers in bioprinting, and may lead to more complex and biomimetic structures.

Incorporating multiple materials also remains a challenge. For most bioprinters, materials to be printed are prepared in bulk before printing begins and switching materials involves changing to secondary pre-loaded reservoirs (e.g. a separate syringe or bioink cartridge). For example, the commercially available 3-D Bioplotter® (EnvisionTEC) is limited to three material cartridges for a single print job. While this approach enables multi-material printing, it makes creating smooth gradients of cells or growth factors impossible or arduous due to the need to prepare many independent solutions. To address this, the Lewis group recently developed an impeller based active mixing system for use in extrusion style printers (Ober et al., 2015). The inclusion of active mixing would reduce the number of solutions that need to be prepared and can enable more precise control over the concentration of deposited components. Although this does introduce some non-trivial complexity to the printing system, the benefits of on the fly mixing are significant. Such a system may also alleviate other concerns for long prints where cell suspensions, pre-polymer solutions, growth factors and other components can be stored in independently controlled reservoirs optimized for their contents.

### 5.2. Future prospects

In the future, bioprinting may be considered as much a nanofabrication technique as a tool for artificial organ generation. Due



to its advantages on the micrometer scale, and highly controllable dispensing of live cells, bioprinting may fill a vital role in biofabrication. Bioprinting can be applied wherever the deposition or integration of live cells is desired. Bio-sensors (Xu et al., 2009a) and protein and DNA arrays of stem cells (Tasoglu and Demirci, 2013) have already been fabricated by bioprinting. These diverse applications illustrate the versatility and potential of bioprinting as a technology still in its infancy. Moreover, bioprinting remains a promising solution for addressing the growing international organ shortage. The ability to generate tissues for transplant on-demand with reduced immune response risk holds significant promise in the fabrication of artificial organs. Recent progress in hydrogel science, including the development of dynamic switchable hydrogels (Gillette et al., 2010) and oxygen producing hydrogels (Harrison et al., 2007), provide researchers with more and more methods to control cell microenvironments. In order to realize the potential of bioprinting and rapid prototyping, the printing speed, characteristics of hydrogels, preparation time for cells and hydrogels, vascularization of tissues, innervation of tissues, and the controllability of on-demand scaffold and cell maturation must be improved further. As the technology matures, bioprinting is poised to become a key technique in the fabrication of human-on-a-chip systems as well as on-demand anatomically realistic artificial organs.

## 6. Conclusions

Bioprinting is an advanced fabrication technique for the dispensing of cell-laden hydrogels, with a bright future accompanying numerous challenges and problems. Bioprinting has shown great potential in tissue engineering applications at its early research stage where many *in vitro* and even *in vivo* experiments have already hinted at the feasibility of bioprinted artificial organs. Due to advantages in micro scale, high-throughput, cell deposition, the applications of bioprinting are expanding rapidly. Bioprinting has become a strong fabrication tool to create complex micro- and macro-scale biomedical systems. Even with the progress that has been made, bioprinting remains an emerging and growing technology with incredible potential.

## Acknowledgement

This work was supported by a National Institutes of Health R21 Grant (R21AR064395) and a Muscular Dystrophy Association Research Grant (MDA255907). This work was also supported by the Natural Sciences and Engineering Research Council of Canada Discovery Grant (Application No. RGPIN-2014-04010)

## References

Abouna, G.M., 2008. Organ shortage crisis: problems and possible solutions. *Transplant. Proc.* 40 (1), 34–38.

Agarwal, S., Greiner, A., Wendorff, J.H., 2013. Functional materials by electrospinning of polymers. *Prog. Polym. Sci.* 38 (6), 963–991.

Arai, K., Iwanaga, S., Toda, H., Genci, C., Nishiyama, Y., Nakamura, M., 2011. Three-dimensional inkjet biofabrication based on designed images. *Biofabrication* 034113.

Araujo, J.V., Davidenko, N., Danner, M., Cameron, R.E., Best, S.M., 2014. Novel porous scaffolds of pH responsive chitosan/carrageenan-based polyelectrolyte complexes for tissue engineering. *J. Biomed. Mater. Res. A* 4415–4426.

Bajaj, P., Schweller, R.M., Khademhosseini, A., West, J.L., Bashir, R., 2014. 3D biofabrication strategies for tissue engineering and regenerative medicine. *Annu. Rev. Biomed. Eng.* 16, 247–276.

Balakrishnan, B., Jayakrishnan, A., Kumar, S.S.P., Nandkumar, A.M., 2012. Anti-bacterial properties of an *in situ* forming hydrogel based on oxidized alginate and gelatin loaded with gentamycin. *Trends Biomater. Artif. Organs* 26 (3), 139–145.

Balint, R., Cassidy, N.J., Cartmell, S.H., 2014. Conductive polymers: towards a smart biomaterial for tissue engineering. *Acta Biomater.* 10 (6), 2341–2353.

Ballins, J.J., Gleghorn, J.P., Niebrzydowski, V., Rawlinson, J.J., Potter, H.G., Maher, S.A., et al., 2008. Image-guided tissue engineering of anatomically shaped implants via MRI and micro-CT using injection molding. *Tissue Eng. A* 14 (7), 1195–1202.

Bauer, M., Kim, K., Qiu, Y., Calpe, B., Khademhosseini, A., Liao, R., et al., 2012. Spot identification and quality control in cell-based microarrays. *ACS Comb. Sci.* 14 (8), 471–477.

Benson, K., Galla, H.J., Kehr, N.S., 2014. Cell adhesion behavior in 3D hydrogel scaffolds functionalized with D- or L-aminoacids. *Macromol. Biosci.* 14 (6), 793–798.

Bertassoni, L.E., Cardoso, J.C., Manoharan, V., Cristino, A.L., Bhise, N.S., Araujo, W.A., et al., 2014a. Direct-write bioprinting of cell-laden methacrylated gelatin hydrogels. *Biofabrication* 6 (2), 024105.

Bertassoni, L.E., Cecconi, M., Manoharan, V., Nikkha, M., Hjortnaes, J., Cristino, A.L., et al., 2014b. Hydrogel bioprinted microchannel networks for vascularization of tissue engineering constructs. *Lab Chip* 14 (13), 2202–2211.

Billiet, T., Vandenhaute, M., Schellhout, J., Van Vlierberghe, S., Dubruel, P., 2012. A review of trends and limitations in hydrogel-rapid prototyping for tissue engineering. *Biomaterials* 6020–6041.

Bohandy, J., Kim, B.F., Adrian, F.J., 1986. Metal deposition from a supported metal film using an excimer laser. *J. Appl. Phys.* 60 (4), 1538–1539.

Bracci, R., Maccaroni, E., Cascinu, S., 2013. Transient sunitinib resistance in gastrointestinal stromal tumors. *N. Engl. J. Med.* 368 (21), 2042–2043.

Burleson, S., Baker, J., Hsia, A.T., Xu, Z., 2015. Use of 3D printers to create a patient-specific 3D bolus for external beam therapy. *J. Appl. Clin. Med. Phys.* 16 (3), 5247.

Catros, S., Fricain, J.-C., Guillotin, B., Pippenger, B., Bareille, R., Remy, M., et al., 2011a. Laser-assisted bioprinting for creating on-demand patterns of human osteoprogenitor cells and nano-hydroxyapatite. *Biofabrication* 3 (2), 025001.

Catros, S., Guillotin, B., Bačáková, M., Fricain, J.C., Guillemot, F., 2011b. Effect of laser energy, substrate film thickness and bioink viscosity on viability of endothelial cells printed by laser-assisted bioprinting. *Appl. Surf. Sci.* 5142–5147.

Chang, C.C., Boland, E.D., Williams, S.K., Hoying, J.B., 2011. Direct-write bioprinting three-dimensional biohybrid systems for future regenerative therapies. *J. Biomed. Mater. Res. B Appl. Biomater.* 160–170.

Chang, R., Emami, K., Wu, H., Sun, W., 2010. Biofabrication of a three-dimensional liver micro-organ as an *in vitro* drug metabolism model. *Biofabrication* 2 (4), 045004.

Cui, X., Breitenkamp, K., Finn, M.G., Lotz, M., D'Lima, D.D., 2012a. Direct human cartilage repair using three-dimensional bioprinting technology. *Tissue Eng. A* 1304–1312.

Cui, X., Breitenkamp, K., Lotz, M., D'Lima, D., 2012b. Synergistic action of fibroblast growth factor-2 and transforming growth factor-beta 1 enhances bioprinted human neocartilage formation. *Biotechnol. Bioeng.* 109 (9), 2357–2368.

Cui, X., Gao, G., Qiu, Y., 2013. Accelerated myotube formation using bioprinting technology for biosensor applications. *Biotechnol. Lett.* 35 (3), 315–321.

Discher, D.E., Janmey, P., Wang, Y.-L., 2005. Tissue cells feel and respond to the stiffness of their substrate. *Science* 310 (5751), 1139–1143.

Dolati, F., Yu, Y., Zhang, Y., De Jesus, A.M., Sander, E.A., Ozbolat, I.T., 2014. *In vitro* evaluation of carbon-nanotube-reinforced bioprintable vascular conduits. *Nanotechnology* 25 (14), 145101.

Dou, X.-Q., Yang, X.-M., Li, P., Zhang, Z.-G., Schönherr, H., Zhang, D., et al., 2012. Novel pH responsive hydrogels for controlled cell adhesion and triggered surface detachment. *Soft Matter* 9539.

Duan, B., Hockaday, L.A., Kang, K.H., Butcher, J.T., 2013. 3D bioprinting of heterogeneous aortic valve conduits with alginate/gelatin hydrogels. *J. Biomed. Mater. Res. A* 101 A (5), 1255–1264.

Duarte Campos, D.F., Blaeser, A., Weber, M., Jäkel, J., Neuss, S., Jahnens-Dechert, W., et al., 2013. Three-dimensional printing of stem cell-laden hydrogels submerged in a hydrophobic high-density fluid. *Biofabrication* 5 (1), 015003.

Duocastella, M., Colina, M., Fernández-Pradas, J.M., Serra, P., Morenza, J.L., 2007. Study of the laser-induced forward transfer of liquids for laser bioprinting. *Appl. Surf. Sci.* 253 (19), 7855–7859.

Gao, H., Sun, L.N., Wu, Y.P., 2012. Preparation and dimming performance study of PNIPAm thermal hydrogel. *Appl. Mech. Mater.* 236–237, 99–104.

Gauvin, R., Chen, Y.-C., Lee, J.W., Soman, P., Zorlutuna, P., Nichol, J.W., et al., 2012. Microfabrication of complex porous tissue engineering scaffolds using 3D projection stereolithography. *Biomaterials* 33 (15), 3824–3834.

Gillette, B.M., Jensen, J.A., Wang, M., Tchao, J., Sia, S.K., 2010. Dynamic hydrogels: switching of 3D microenvironments using two-component naturally derived extracellular matrices. *Adv. Mater.* 22 (6), 686–691.

Glowacki, J., Mizuno, S., 2008. Collagen scaffolds for tissue engineering. *Biopolymers* 89 (5), 338–344.

Gou, M., Qu, X., Zhu, W., Xiang, M., Yang, J., Zhang, K., et al., 2014. Bio-inspired detoxification using 3D-printed hydrogel nanocomposites. *Nat. Commun.* 5, 3774.

Grogan, S.P., Chung, P.H., Soman, P., Chen, P., Lotz, M.K., Chen, S., et al., 2013. Digital micromirror device projection printing system for meniscus tissue engineering. *Acta Biomater.* 9 (7), 7218–7226.

Gruene, M., Pflaum, M., Deiwick, A., Koch, L., Schlie, S., Unger, C., et al., 2011a. Adipogenic differentiation of laser-printed 3D tissue grafts consisting of human adipose-derived stem cells. *Biofabrication* 3 (1), 015005.

Gruene, M., Unger, C., Koch, L., Deiwick, A., Chichkov, B., 2011b. Dispensing pico to nanoliter of a natural hydrogel by laser-assisted bioprinting. *Biomed. Eng. Online* 10 (1), 19.

Guillemot, F., Souquet, A., Catros, S., Guillotin, B., Lopez, J., Faucon, M., et al., 2010. High-throughput laser printing of cells and biomaterials for tissue engineering. *Acta Biomater.* 2494–2500.

Guillot, B., Souquet, A., Catros, S., Duocastella, M., Pippenger, B., Bellance, S., et al., 2010. Laser assisted bioprinting of engineered tissue with high cell density and microscale organization. *Biomaterials* 31 (28), 7250–7256.

Harrison, B.S., Eberli, D., Lee, S.J., Atala, A., Yoo, J.J., 2007. Oxygen producing biomaterials for tissue regeneration. *Biomaterials* 28 (31), 4628–4634.

Hinton, T.J., Jallerat, Q., Palchesko, R.N., Park, J.H., Grodzicki, M.S., Shue, H.-J., et al., 2015. Three-dimensional printing of complex biological structures by freeform reversible embedding of suspended hydrogels. *Sci. Adv.* 1 (9), e1500758.

Hobkirk, J.A., 1988. Definitions in biomaterials. *Clin. Mater.* 261.



- Hong, S., Song, S.J., Lee, J.Y., Jang, H., Choi, J., Sun, K., et al., 2013. Cellular behavior in micropatterned hydrogels by bioprinting system depended on the cell types and cellular interaction. *J. Biosci. Bioeng.* 116 (2), 224–230.
- Hsu, A.R., Ellington, J.K., 2015. Patient-specific 3-dimensional printed titanium truss cage with tibialocalcaneal arthrodesis for salvage of persistent distal tibia nonunion. *Foot Ankle Spec.*
- Huang, T.Q., Qu, X., Liu, J., Chen, S., 2014. 3D printing of biomimetic microstructures for cancer cell migration. *Biomed. Microdevices* 16 (1), 127–132.
- Huh, D.D., Kim, D.-H., 2015. JALA special issue: microengineered cell- and tissue-based assays for drug screening and toxicology applications. *J. Lab. Autom.* 20 (2), 79–81.
- Hutmacher, D.W., 2000. Scaffolds in tissue engineering bone and cartilage. *Biomaterials* 21 (24), 2529–2543.
- Jakus, A.E., Secor, E.B., Rutz, A.L., Jordan, S.W., Hersam, M.C., Shah, R.N., 2015. Three-dimensional printing of high-content graphene scaffolds for electronic and biomedical applications. *ACS Nano* 9 (4), 4636–4648.
- Jiao, A., Trosper, N.E., Yang, H.S., Kim, J., Tsui, J.H., Frankel, S.D., et al., 2014. Thermoresponsive nanofabricated substratum for the engineering of three-dimensional tissues with layer-by-layer architectural control. *ACS Nano* 8, 4430–4439.
- Kattamis, N.T., Purnick, P.E., Weiss, R., Arnold, C.B., 2007. Thick film laser induced forward transfer for deposition of thermally and mechanically sensitive materials. *Appl. Phys. Lett.* 91 (17), 171120.
- Ker, E.D.F., Nain, A.S., Weiss, L.E., Wang, J., Suhan, J., Amon, C.H., et al., 2011. Bioprinting of growth factors onto aligned sub-micron fibrous scaffolds for simultaneous control of cell differentiation and alignment. *Biomaterials* 32 (32), 8097–8107.
- Keriquel, V., Guillemot, F., Arnault, I., Guillotin, B., Miraux, S., Amédée, J., et al., 2010. In vivo bioprinting for computer- and robotic-assisted medical intervention: preliminary study in mice. *Biofabrication* 2 (1), 014101.
- Khademhosseini, A., Langer, R., Borenstein, J., Vacanti, J.P., 2006. Tissue engineering special feature: microscale technologies for tissue engineering and biology. *Proc. Natl. Acad. Sci.* 103 (8), 2480–2487.
- Khalil, S., Sun, W., 2007. Biopolymer deposition for freeform fabrication of hydrogel tissue constructs. *Mater. Sci. Eng. C* 27 (3), 469–478.
- Khalil, S., Sun, W., 2009. Bioprinting endothelial cells with alginate for 3D tissue constructs. *J. Biomech. Eng.* 131 (11), 111002.
- Kim, E.-S., Ahn, E.H., Dvir, T., Kim, D.-H., 2014a. Emerging nanotechnology approaches in tissue engineering and regenerative medicine. *Int. J. Nanomedicine* 9 (Suppl. 1), 1–5.
- Kim, H.N., Jiao, A., Hwang, N.S., Kim, M.S., Kang, D.H., Kim, D.-H., et al., 2013. Nanotopography-guided tissue engineering and regenerative medicine. *Adv. Drug Deliv. Rev.* 65 (4), 536–558.
- Kim, H.N., Kang, D.-H., Kim, M.S., Jiao, A., Kim, D.-H., Suh, K.-Y., 2012. Patterning methods for polymers in cell and tissue engineering. *Ann. Biomed. Eng.* 40 (6), 1339–1355.
- Kim, D.-H., Lipke, E.A., Kim, P., Cheong, R., Thompson, S., Delannoy, M., et al., 2010. Nanoscale cues regulate the structure and function of macroscopic cardiac tissue constructs. *Proc. Natl. Acad. Sci. U. S. A.* 107, 565–570.
- Kim, P., Yuan, A., Nam, K.-H., Jiao, A., Kim, D.-H., 2014b. Fabrication of poly(ethylene glycol): gelatin methacrylate composite nanostructures with tunable stiffness and degradation for vascular tissue engineering. *Biofabrication* 6, 024112.
- Kolesky, D.B., Truby, R.L., Gladman, A.S., Busbee, T.A., Homan, K.A., Lewis, J.A., 2014. 3D bioprinting of vascularized, heterogeneous cell-laden tissue constructs. *Adv. Mater.* 26 (19), 3124–3130.
- Kundu, J., Shim, J.-H., Jang, J., Kim, S.-W., Cho, D.-W., 2013. An additive manufacturing-based PCL-alginate-chondrocyte bioprinted scaffold for cartilage tissue engineering. *J. Tissue Eng. Regen. Med.*
- Langer, R., Vacanti, J.P., 1993. Tissue engineering. *Science* 260 (5110), 920–926.
- Lee, J.-S., Hong, J.M., Jung, J.W., Shim, J.-H., Oh, J.-H., Cho, D.-W., 2014. 3D printing of composite tissue with complex shape applied to ear regeneration. *Biofabrication* 6 (2), 024103.
- Li, Z., Ramay, H.R., Hauch, K.D., Xiao, D., Zhang, M., 2005. Chitosan-alginate hybrid scaffolds for bone tissue engineering. *Biomaterials* 26 (18), 3919–3928.
- Limpanuphap, S., Derby, B., 2002. Manufacture of biomaterials by a novel printing process. *J. Mater. Sci. Mater. Med.* 1163–1166.
- Liu, X., Smith, L.A., Hu, J., Ma, P.X., 2009. Biomimetic nanofibrous gelatin/apatite composite scaffolds for bone tissue engineering. *Biomaterials* 30 (12), 2252–2258.
- Loozen, L.D., Wegman, F., Öner, F.C., Dhert, W.J.A., Alblas, J., 2013. Porous bioprinted constructs in BMP-2 non-viral gene therapy for bone tissue engineering. *J. Mater. Chem. B* 1 (48), 6619.
- Lorber, B., Hsiao, W.-K., Hutchings, I.M., Martin, K.R., 2014. Adult rat retinal ganglion cells and glia can be printed by piezoelectric inkjet printing. *Biofabrication* 6 (1), 015001.
- Lu, T., Li, Y., Chen, T., 2013. Techniques for fabrication and construction of three-dimensional scaffolds for tissue engineering. *Int. J. Nanomedicine* 8, 337–350.
- Markstedt, K., Mantas, A., Tournier, I., Martínez Ávila, H., Hägg, D., Gatenholm, P., 2015. 3D bioprinting human chondrocytes with nanocellulose-alginate bioink for cartilage tissue engineering applications. *Biomacromolecules* 16 (5), 1489–1496.
- Mattimore, J.P., Groff, R.E., Burg, T., Pepper, M.E., 2010. A general purpose driver board for the HP26 ink-jet cartridge with applications to bioprinting. *Conf Proc - IEEE SOUTHEASTCON*, pp. 510–513.
- McCune, M., Shafiee, A., Forgacs, G., Kosztin, I., 2014. Predictive modeling of post bioprinting structure formation. *Soft Matter* 10 (11), 1790.
- Merceron, T.K., Burt, M., Seol, Y.-J., Kang, H.-W., Lee, S.J., Yoo, J.J., et al., 2015. A 3D bioprinted complex structure for engineering the muscle-tendon unit. *Biofabrication* 7 (3), 035003.
- Mézel, C., Souquet, A., Hallo, L., Guillemot, F., 2010. Bioprinting by laser-induced forward transfer for tissue engineering applications: jet formation modeling. *Biofabrication* 2 (1), 014103.
- Michael, S., Sorg, H., Peck, C.T., Koch, L., Deiwick, A., Chichkov, B., et al., 2013. Tissue engineered skin substitutes created by laser-assisted bioprinting form skin-like structures in the dorsal skin fold chamber in mice. *PLoS ONE* 8 (3), e57741.
- Miller, J.S., Stevens, K.R., Yang, M.T., Baker, B.M., Nguyen, D.T., Cohen, D.M., et al., 2012. Rapid casting of patterned vascular networks for perfusable engineered three-dimensional tissues. *Nat. Mater.* 11 (9), 768–774.
- Mironov, V., Kasyanov, V., Markwald, R.R., 2008. Nanotechnology in vascular tissue engineering: from nanoscaffolding towards rapid vessel biofabrication. *Trends Biotechnol.* 338–344.
- Mironov, V., Zhang, J., Gentile, C., Brakke, K., Trusk, T., Jakab, K., et al., 2009. Designer “blueprint” for vascular trees: morphology evolution of vascular tissue constructs. *Virtual Phys. Prototyp.* 63–74.
- Mobed-Miremadi, M., Asi, B., Parasseri, J., Wong, E., Tat, M., Shan, Y., 2012. Comparative diffusivity measurements for alginate-based atomized and inkjet-bioprinted artificial cells using fluorescence microscopy. *Artif. Cells, Blood Substit. Biotechnol.* 41 (3), 1–6.
- Mondy, W.L., Cameron, D., Timmermans, J.-P., De Clerck, N., Sasov, A., Casteleyn, C., et al., 2009. Computer-aided design of microvasculature systems for use in vascular scaffold production. *Biofabrication* 1 (3), 035002.
- Murphy, S.V., Atala, A., 2014. 3D bioprinting of tissues and organs. *Nat. Biotechnol.* 32 (8), 773–785.
- Murphy, S.V., Skardal, A., Atala, A., 2013. Evaluation of hydrogels for bio-printing applications. *J. Biomed. Mater. Res. A* 101 A (1), 272–284.
- Nahmias, Y., Schwartz, R.E., Verfaillie, C.M., Odde, D.J., 2005. Laser-guided direct writing for three-dimensional tissue engineering. *Biotechnol. Bioeng.* 92 (2), 129–136.
- Nam, K.-H., Smith, A.S.T., Lone, S., Kwon, S., Kim, D.-H., 2015. Biomimetic 3D tissue models for advanced high-throughput drug screening. *J. Lab. Autom.* 20 (3), 201–215.
- Nichol, J.W., Koshy, S.T., Bae, H., Hwang, C.M., Yamanlar, S., Khademhosseini, A., 2010. Cell-laden microengineered gelatin methacrylate hydrogels. *Biomaterials* 31 (21), 5536–5544.
- Nikkhah, M., Eshak, N., Zorlutuna, P., Annabi, N., Castello, M., Kim, K., et al., 2012. Directed endothelial cell morphogenesis in micropatterned gelatin methacrylate hydrogels. *Biomaterials* 33 (35), 9009–9018.
- Nishiyama, Y., Nakamura, M., Henmi, C., Yamaguchi, K., Mochizuki, S., Nakagawa, H., et al., 2009. Development of a three-dimensional bioprinter: construction of cell supporting structures using hydrogel and state-of-the-art inkjet technology. *J. Biomech. Eng.* 131 (3), 035001.
- Ober, T.J., Foresti, D., Lewis, J.A., 2015. Active mixing of complex fluids at the microscale. *Proc. Natl. Acad. Sci. U. S. A.* 112 (40), 12293–12298.
- Orloff, N.D., Truong, C., Cira, N.J., Koo, S., Hamilton, A.L., Choi, S., et al., 2014. Integrated bioprinting and imaging for scalable, networkable desktop experimentation. *RSC Adv.* 4 (65), 34721.
- Ousterout, D.G., Perez-Pinera, P., Thakore, P.I., Kabadi, A.M., Brown, M.T., Qin, X., et al., 2013. Reading frame correction by targeted genome editing restores dystrophin expression in cells from Duchenne muscular dystrophy patients. *Mol. Ther.* 21 (9), 1718–1726.
- Owens, C.M., Marga, F., Forgacs, G., Heesch, C.M., 2013. Biofabrication and testing of a fully cellular nerve graft. *Biofabrication* 5 (4), 045007.
- Ozbolat, I.T., Yu, Y., 2013. Bioprinting toward organ fabrication: challenges and future trends. *IEEE Trans. Biomed. Eng.* 60 (3), 691–699.
- Ozbolat, I.T., Chen, H., Yu, Y., 2014. Development of “multi-arm bioprinter” for hybrid bioprinting of tissue engineering constructs. *Robot. Comput. Integr. Manuf.* 30 (3), 295–304.
- Pateman, C.J., Harding, A.J., Glen, A., Taylor, C.S., Christmas, C.R., Robinson, P.P., et al., 2015. Nerve guides manufactured from photocurable polymers to aid peripheral nerve repair. *Biomaterials* 49, 77–89.
- Pati, F., Jang, J., Ha, D.-H., Won Kim, S., Rhie, J.-W., Shim, J.-H., et al., 2014. Printing three-dimensional tissue analogues with decellularized extracellular matrix bioink. *Nat. Commun.* 5, 3935.
- Pati, F., Song, T.-H., Rijal, G., Jang, J., Kim, S.W., Cho, D.-W., 2015. Ornamenting 3D printed scaffolds with cell-laid extracellular matrix for bone tissue regeneration. *Biomaterials* 37, 230–241.
- Pepper, M.E., Seshadri, V., Burg, T.C., KJL, B., Groff, R.E., 2012. Characterizing the effects of cell settling on bioprinter output. *Biofabrication* 011001.
- Pepper, M.E., Seshadri, V., Burg, T., Booth, B.W., KJL, B., Groff, R.E., 2011. Cell settling effects on a thermal inkjet bioprinter. *Proc Annu Int Conf IEEE Eng Med Biol Soc EMBS*, pp. 3609–3612.
- Pietrabissa, A., Marconi, S., Peri, A., Pugliese, L., Cavazzi, E., Vinci, A., et al., 2015. From CT scanning to 3-D printing technology for the preoperative planning in laparoscopic splenectomy. *Surg. Endosc.*
- Scawn, R.L., Foster, A., Lee, B.W., Kikkawa, D.O., Korn, B.S., 2015. Customised 3D printing: an innovative training tool for the next generation of orbital surgeons. *Orbit* 1–4.
- Schuurman, W., Khristov, V., Pot, M.W., van Weeren, P.R., Dhert, W.J.A., Malda, J., 2011. Bioprinting of hybrid tissue constructs with tailorable mechanical properties. *Biofabrication* 3 (2), 021001.
- Shapira, A., Kim, D.-H., Dvir, T., 2014. Advanced micro- and nanofabrication technologies for tissue engineering. *Biofabrication* 6 (2), 020301.
- Shin, S.R., Jung, S.M., Zalabany, M., Kim, K., Zorlutuna, P., Kim, S.B., et al., 2013. Carbon-nanotube-embedded hydrogel sheets for engineering cardiac constructs and bioactuators. *ACS Nano* 7 (3), 2369–2380.
- Sim, J.H., Puria, S., Steele, C.R., 2007. *Mech. Mater. Struct.* 2 (October).
- Singh, M., Haverinen, H.M., Dhagat, P., Jabbour, G.E., 2010. Inkjet printing-process and its applications. *Adv. Mater.* 22 (6), 673–685.
- Skardal, A., Atala, A., 2014. Biomaterials for integration with 3-D bioprinting. *Ann. Biomed. Eng.* 43 (3), 730–746.

- Snyder, J.E., Hamid, Q., Wang, C., Chang, R., Emami, K., Wu, H., et al., 2011. Bioprinting cell-laden Matrigel for radioprotection study of liver by pro-drug conversion in a dual-tissue microfluidic chip. *Biofabrication* 3 (3), 034112.
- Sun, Y., Wang, Q., 2013. Modeling and simulations of multicellular aggregate self-assembly in biofabrication using kinetic Monte Carlo methods. *Soft Matter* 9 (7), 2172.
- Talelli, M., Rijcken, C.J.F., Lammers, T., Seevinck, P.R., Storm, G., Van Nostrum, C.F., et al., 2009. Superparamagnetic iron oxide nanoparticles encapsulated in biodegradable thermosensitive polymeric micelles: toward a targeted nanomedicine suitable for image-guided drug delivery. *Langmuir* 25 (4), 2060–2067.
- Tasoglu, S., Demirci, U., 2013. Bioprinting for stem cell research. *Trends Biotechnol.* 10–19.
- Tatman, P.D., Gerull, W., Sweeney-Easter, S., Davis, J.L., Kim, D.-H., Gee, A., 2015. Multi-scale biofabrication of articular cartilage: bioinspired and biomimetic approaches. *Tissue Eng. B Rev.*
- Taylor, R.E., Kim, K., Sun, N., Park, S.J., Sim, J.Y., Fajardo, G., et al., 2013. Sacrificial layer technique for axial force post assay of immature cardiomyocytes. *Biomed. Microdevices* 15 (1), 171–181.
- Thomas, G.L., Mironov, V., Nagy-Mehez, A., Mombach, J.C.M., 2014. Dynamics of cell aggregates fusion: experiments and simulations. *Phys. A Stat. Mech. Appl.* 395, 247–254.
- Tirella, A., Vozzi, F., De Maria, C., Vozzi, G., Sandri, T., Sassano, D., et al., 2011. Substrate stiffness influences high resolution printing of living cells with an ink-jet system. *J. Biosci. Bioeng.* 112 (1), 79–85.
- Tuan, R.S., Boland, G., Tuli, R., 2003. Adult mesenchymal stem cells and cell-based tissue engineering. *Arthritis Res. Ther.* 5 (1), 32–45.
- Tumbleston, J.R., Shirvanyants, D., Ermoshkin, N., Januszewicz, R., Johnson, A.R., Kelly, D., et al., 2015. Continuous liquid interface production of 3D objects. *Science* 347 (6228), 1349–1352 (80- ).
- Villar, G., Graham, A.D., Bayley, H., 2013. A tissue-like printed material. *Science* 340 (6128), 48–52.
- Visser, J., Peters, B., Burger, T.J., Boomstra, J., Dhert, W.J.A., FPW, M., et al., 2013. Biofabrication of multi-material anatomically shaped tissue constructs. *Biofabrication* 5 (3), 035007.
- Wang, M.O., Piard, C.M., Melchiorri, A., Dreher, M.L., Fisher, J.P., 2015a. Evaluating changes in structure and cytotoxicity during in vitro degradation of three-dimensional printed scaffolds. *Tissue Eng. A* 21 (9–10), 1642–1653.
- Wang, Z., Roy, S., Kyo-in, K., Kim, K., 2015b. Organ-on-a-chip platforms for drug delivery and cell characterization: a review. *Sens. Mater.* 27 (6), 487–506.
- Wang, Z., Abdulla, R., Parker, B., Samanipour, R., Ghosh, S., Kim, K., 2015c. A simple and high-resolution stereolithography-based 3D bioprinting system using visible light crosslinkable bioinks. *Biofabrication* 7 (4), 045009.
- Weiner, A.A., Shuck, D.M., Bush, J.R., Prasad Shastri, V., 2007. In vitro degradation characteristics of photocrosslinked anhydride systems for bone augmentation applications. *Biomaterials* 28 (35), 5259–5270.
- Weiss, L.E., Amon, C.H., Finger, S., Miller, E.D., Romero, D., Verdinelli, I., et al., 2005. Bayesian computer-aided experimental design of heterogeneous scaffolds for tissue engineering. *Comput. Aided Des.* 37 (11), 1127–1139.
- Williams, D.F., 2008. On the mechanisms of biocompatibility. *Biomaterials* 29 (20), 2941–2953.
- Wu, Y., Wei, W., Zhou, M., Wang, Y., Wu, J., Ma, G., et al., 2012. Thermal-sensitive hydrogel as adjuvant-free vaccine delivery system for H5N1 intranasal immunization. *Biomaterials* 33 (7), 2351–2360.
- Xu, T., Baicu, C., Aho, M., Zile, M., Boland, T., 2009b. Fabrication and characterization of bio-engineered cardiac pseudo tissues. *Biofabrication* 1 (3), 035001.
- Xu, T., Binder, K.W., Albanna, M.Z., Dice, D., Zhao, W., Yoo, J.J., et al., 2013. Hybrid printing of mechanically and biologically improved constructs for cartilage tissue engineering applications. *Biofabrication* 5 (1), 015001.
- Xu, C., Chai, W., Huang, Y., Markwald, R.R., 2012. Scaffold-free inkjet printing of three-dimensional zigzag cellular tubes. *Biotechnol. Bioeng.* 109 (12), 3152–3160.
- Xu, T., Jin, J., Gregory, C., Hickman, J.J., Boland, T., 2005. Inkjet printing of viable mammalian cells. *Biomaterials* 26 (1), 93–99.
- Xu, F., Moon, S., Emre, A.E., Lien, C., Turali, E.S., Demirci, U., 2009a. Cell bioprinting as a potential high-throughput method for fabricating cell-based biosensors (CBBs). *Proc IEEE Sensors*, pp. 387–391.
- Xu, F., Sridharan, B., Wang, S., Gurkan, U.A., Syverud, B., Demirci, U., 2011. Embryonic stem cell bioprinting for uniform and controlled size embryoid body formation. *Biomicrofluidics* 5 (2), 22207.
- Yang, X., Mironov, V., Wang, Q., 2012. Modeling fusion of cellular aggregates in biofabrication using phase field theories. *J. Theor. Biol.* 303, 110–118.
- Yang, X., Sun, Y., Wang, Q., 2013. A phase field approach for multicellular aggregate fusion in biofabrication. *J. Biomech. Eng.* 135 (7), 71005.
- Yao, Q., Wei, B., Guo, Y., Jin, C., Du, X., Yan, C., et al., 2015. Design, construction and mechanical testing of digital 3D anatomical data-based PCL-HA bone tissue engineering scaffold. *J. Mater. Sci. Mater. Med.* 26 (1), 5360.
- Yu, Y., Zhang, Y., Martin, J.A., Ozbolat, I.T., 2013. Evaluation of cell viability and functionality in vessel-like bioprintable cell-laden tubular channels. *J. Biomech. Eng.* 135 (9), 91011.
- Zhang, H., Xu, K., Ai, H., Chen, D., Xv, L., Chen, M., 2008. Synthesis, characterization and solution properties of hydrophobically modified polyelectrolyte poly(AA-co-TMSPMA). *J. Solut. Chem.* 37 (8), 1137–1148.
- Zhang, X., Xu, B., Puperi, D.S., Yonezawa, A.L., Wu, Y., Tseng, H., et al., 2015. Integrating valve-inspired design features into poly(ethylene glycol) hydrogel scaffolds for heart valve tissue engineering. *Acta Biomater.* 14, 11–21.
- Zhang, T., Yan, K.C., Ouyang, L., Sun, W., 2013. Mechanical characterization of bioprinted in vitro soft tissue models. *Biofabrication* 5 (4), 045010.
- Zhao, Y., Yao, R., Ouyang, L., Ding, H., Zhang, T., Zhang, K., et al., 2014. Three-dimensional printing of HeLa cells for cervical tumor model in vitro. *Biofabrication* 6 (3), 035001.
- Zheng, Y., Chen, J., Craven, M., Choi, N.W., Totorica, S., Diaz-Santana, A., et al., 2012. In vitro microvessels for the study of angiogenesis and thrombosis. *Proc. Natl. Acad. Sci. U. S. A.* 109 (24), 9342–9347.
- Zhu, J., Marchant, R.E., 2011. Design properties of hydrogel tissue-engineering scaffolds. *Expert Rev. Med. Devices* 8 (5), 607–626.
- Zorlutuna, P., Vrana, N.E., Khademhosseini, A., 2013. The expanding world of tissue engineering: the building blocks and new applications of tissue engineered constructs. *IEEE Rev. Biomed. Eng.* 6, 47–62.
- Zustiak, S.P., Leach, J.B., 2010. Hydrolytically degradable poly(ethylene glycol) hydrogel scaffolds with tunable degradation and mechanical properties. *Biomacromolecules* 11 (5), 1348–1357.